BIOCHEMISTRY
including biophysical chemistry & molecular biology
Article

Biochemistry **2010,** *49,* 10747–10755 10747
DOI: 10.1021/bi1013003

Seipin Is a Discrete Homooligomer[†]

Derk Binns,[‡] SungKyung Lee,[‡] Christopher L. Hilton,[‡] Qiu-Xing Jiang,[§] and Joel M. Goodman*[,‡]

[‡]*Departments of Pharmacology and* [§]*Cell Biology, The University of Texas Southwestern Medical Center, Dallas, Texas 75390, United States*

Received August 13, 2010; Revised Manuscript Received November 3, 2010

ABSTRACT: Seipin is a transmembrane protein that resides in the endoplasmic reticulum and concentrates at junctions between the ER and cytosolic lipid droplets. Mutations in the human seipin gene, including the missense mutation A212P, lead to congenital generalized lipodystrophy (CGL), characterized by the lack of normal adipose tissue and accumulation of fat in liver and muscles. In both yeast and CGL patient fibroblasts, seipin is required for normal lipid droplet morphology; in its absence droplets appear to bud abnormally from the ER. Here we report the first purification and physical characterization of seipin. Yeast seipin is in a large discrete protein complex. Affinity purification demonstrated that seipin is the main if not exclusive protein in the complex. Detergent sucrose gradients in H_2O, and D_2O and gel filtration were used to determine the size of the seipin complex and account for detergent binding. Both seipin-myc13 (seipin fused to 13 tandem copies of the myc epitope) expressed from the endogenous promoter and overexpressed seipin-mCherry form ~500 kDa proteins consisting of about 9 copies of seipin. The yeast orthologue of the human A212P allele forms only smaller complexes and is unstable; we hypothesize that this accounts for its null phenotype in humans. Seipin appears as a toroid by negative staining electron microscopy. We speculate that seipin plays at least a structural role in organizing droplets or in communication between droplets and ER.

Congenital generalized lipodystrophy is characterized by the inability to develop adipose tissue. In extreme cases this syndrome results in several metabolic abnormalities and diabetes caused by the lack of adipokines. Patients are hyperphagic leading to fat accumulation in the liver and muscles; the cause of death is often liver failure at an early age (*1*, *2*). Recently, there has been some success in treating lipodystrophy patients with leptin (*3*).

The severest form of lipodystrophy, congenital generalized lypodystrophy type 2 (CGL2),[1] is caused by mutations in the BSCL2 gene encoding seipin (*4*). Seipin is normally expressed in fat, but mRNA levels are highest in the nervous system and testes (*4*). It is an endoplasmic reticulum- (ER-) resident protein that concentrates at the junction of cytoplasmic lipid droplets (*5*−*7*). Seipins from fungi, animals, and plants share a core structure consisting of two likely transmembrane domains with a ER luminal loop that is glycosylated in mammals (*6*, *8*); according to this topological model, both termini face the cytosol (*9*).

How mutations in seipin result in the lack of adipogenesis in patients is unknown. CGL2 is recessive, so it is presumed to be caused by a loss of function, and all but one allele contain nonsense mutations; in contrast, mutations in the glycosylation site are dominant and result in neuropathies (*7*, *8*). Seipin knockdown in cultured adipogenic cell lines results in disruption of adipogenesis, mimicking lipodystrophy, although the step in the pathway affected is different in the studies (*10*, *11*). However, in both *Saccharomyces cerevisiae* disrupted in the seipin gene (*FLD1*) and fibroblasts from a CGL2 patient, cytoplasmic lipid droplets appear very disorganized and seem to bud chaotically from the ER (*6*). In yeast the droplets have fusogenic properties in vivo and in vitro (*5*). Abnormalities in fatty acid composition of phospholipids in yeast and cells from a CGL2 patient also have been observed (*5*, *12*).

While most CGL2 patients have null alleles for seipin, a few have an A212P missense mutation in the loop domain (*4*). Human seipin can complement a yeast *FLD1* knockout, but neither the human A212P mutation nor the orthologous G225P *FLD1* mutation is functional in this background (*5*, *6*). It is unknown how this point mutation within the loop region leads to a nonfunctional protein.

To gain insight into seipin function, we searched for binding partners. Although none were found from Triton X-100 solubilized membrane extracts, we found that seipin is a homooligomer of about nine subunits with a radially symmetric shape. This shape, along with its apparent importance in droplet formation, suggests that one role of seipin may be to form a collar to organize droplet assembly.

EXPERIMENTAL PROCEDURES

Strains and Growth Conditions. *S. cerevisiae* strain BY4742 (Open Biosystems) was the parent strain for all strain constructions and experiments. Strains used in this study are listed and described in Table 1. A high-efficiency transformation protocol (*13*) was used to introduce DNA into yeast, and prototrophic transformants were selected on the appropriate nutrient dropout plates. PCR was used to confirm homologous integration of all knock-in constructs. Cells were cultured in minimal synthetic growth medium (yeast nitrogen base (Difco), 2% dextrose, and appropriate base and amino acid supplements). Liquid cultures were incubated at 30 °C in a rotary shaker at 210 rpm. A 50 mL starter culture from a plate was grown for 24 h. Cells were harvested and diluted into 500 mL of fresh medium and grown

[†]This work was financially supported by the NIH (GM08210 to J.M.G., GM088745 to Q.-X.J.) and The Welch Foundation (I-684 to Q.-X.J.).

*To whom correspondence should be addressed. Phone: (214) 645-6139. Fax: (214) 645-6139. E-mail: Joel.Goodman@UTSouthwestern.edu.

[1]Abbreviations: CGL2, congenital lipodystrophy type 2; ER, endoplasmic reticulum; TEV, tobacco etch virus.

© 2010 American Chemical Society

Published on Web 11/09/2010

Table 1: Plasmids and Strains Used in This Study

plasmids	
pDB1	pRS313 (*39*) with the following insert: *PGK1* promoter, *FLD1* ORF fused with myc13 (13 tandem copies of myc epitope), PGK1 term
pDB2	pRS315 (*39*) with the following insert: *PGK1* promoter, *FLD1* ORF with G225 codon mutated from GGG to CCG generating G225P, fused with mCherry, PGK1 term
pDB3	pRS313 with the following insert: *PGK1* promoter, *FLD1* ORF fused with tobacco etch virus protease site (coding for ENLYFQG) and myc13 (13 tandem copies of myc epitope), *PGK1* term
strains[a]	
seipin-myc13 OE	BY4742 *fld1*Δ::kan^R with pDB1 plasmid
seipin-myc13	BY4742 *fld1*Δ::*FLD1* ORF fused to myc13 followed by *TADH1* term and *HIS3*
seipin[G225P]-myc13	identical to seipin-myc13 strain except G225 codon GGG in *FLD1* ORF replaced with CCG yielding G225P
seipin OE	described in Szymanski et al. (*6*)
seipin[G225P] OE	described in Szymanski et al. (*6*)
seipin-mCherry OE	described in Szymanski et al. (*6*)
seipin[G225P]-mCherry OE	BY4742; *fld1*Δ::kan^R with pDB2 plasmid
seipin-TEV-myc13 OE	BY4742; *fld1*Δ::kan^R with pDB3 plasmid

[a]All strains based on BY4742 (MATα his3Δ1 leu2Δ0 lys2Δ0 ura3Δ0) or BY4742 *fld1*Δ::kan^R as indicated (Open Biosystems).

overnight again. Finally, the overnight culture was harvested and diluted into 2750 mL of medium and cultured for 5−5.5 h before use.

Reagents. The monoclonal anti-myc antibody 9E10 was purchased from the National Cell Culture Center (Minneapolis, MN) and the Living Colors DsRed polyclonal antibody, used to detect mCherry on blots, was from Clontech. Deuterium oxide was purchased from Sigma Aldrich. Molecular biology enzymes were purchased from New England Biolabs, the rapid DNA ligation kit was from Roche, and the HotStar HiFidelity polymerase kit was from Qiagen. Sephacryl S-500 high resolution was from GE Healthcare, and dextran from *Leuconostoc mesenteroides* (MW 5−40 MDa) was from Sigma. The Pierce coimmunoprecipitation kit was from Thermo Scientific. All chemicals were of reagent grade. *Escherichia coli* 70s ribosomes were from the Dunkle laboratory (UC Berkeley). Standard 40 nm nanobeads were purchased from Polysciences, Inc. (www.polysciences.com). A polyclonal antibody against yeast seipin (amino acids 165−178, preceded by a cysteine residue) was generated by GenScript Corp. (www.genscript.com) from a synthetic peptide and affinity purified.

Plasmid Constructions. A list and description of plasmids used in this study are in Table 1. Details of the constructions are available upon request. All PCR-generated and mutagenesis constructs introduced into yeast were confirmed by sequencing.

Seipin Stability. To compare the stability of seipin with seipin-[G225P] we used the untagged overexpressed forms. (Untagged seipin expressed from the endogenous promoter cannot be detected with our antibody, and a tag was avoided since it partially stabilizes the protein (Figure 1A).) The experiment using MG132 closely followed a previously published method (*14*) except the time course after addition of cycloheximide was from 0 to 6 h. Intact cells were processed by lysis in base (*15*), and samples were immunoblotted with anti-seipin antibody.

Preparation of ER-Enriched Membranes. Membranes were prepared based on a published method (Preparation of Microsomes from ref *16*) with several modifications: Spheroplasts were generated with Zymolyase 100T in the following buffer: 10 mM Tris-HCl, pH 7.4, 0.7 M sorbitol, 0.5% glucose, 0.75% yeast extract, 1.5% bacto-peptone, and 1 mM DTT. Spheroplast lysis buffer consisted of 20 mM HEPES/KOH, pH 7.4, 50 mM potassium acetate, 0.2 M sorbitol, and 2 mM EDTA. Before freezing, cells were resuspended at 500 OD_{600}/mL in spheroplast lysis buffer with the following protease inhibitors: 0.4 mM 4-(2-aminoethyl)-benzenesulfonyl fluoride hydrochloride, 10 μg/mL aprotinin,

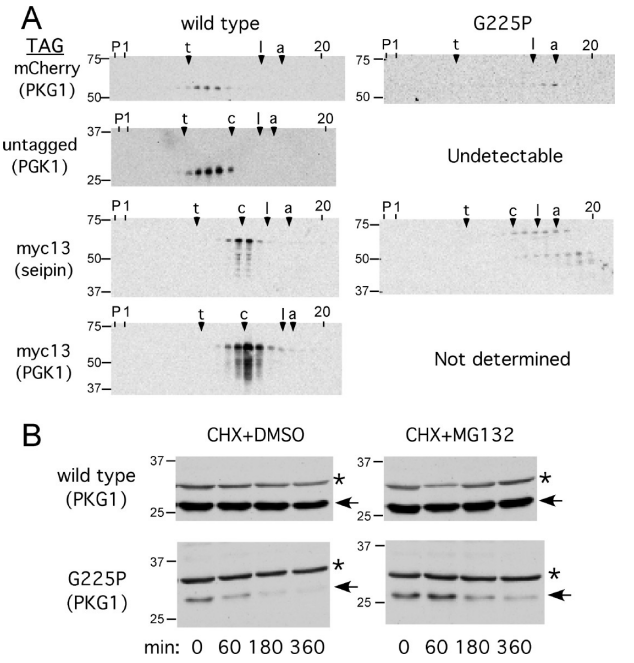

FIGURE 1: Wild-type and mutant seipins migrate as discrete oligomers. (A) Immunoblots of fractions from detergent glycerol gradients. Columns indicate wild-type or G225P seipin sequence, rows indicate the carboxy-terminal tag of the fusion protein, which is driven either by the *PGK1* promoter on a plasmid or by the endogenous chromsosomal seipin promoter, as indicated by parentheses. For each blot the positions of the pellet, first, and twentieth fraction (from bottom to top of gradient) are indicated. Arrowheads denote the position of internal native standards as determined by densitometry of Amido Black-stained nitrocellulose used later for the immunoblots. The standards are as follows: t, thyroglobulin (669 kDa); c, catalase (232 kDa), not included for mCherry constructs due to cross-reactivity with the antibody; l, lactate dehydrogenase (140 kDa); and a, albumin (67 kDa). The nitrocellulose was immunoblotted for mCherry (first row), seipin (second row), or myc (third and fourth rows). Prestained molecular mass markers (kDa) are shown to the left of panels. (B) Seipin[G225P] is unstable. Cells overexpressing untagged wild-type or seipin[G225P] were subjected to cycloheximide (CHX) in the presence of the proteosomal inhibitor MG132 or its vehicle DMSO. Cells were lysed at the times indicated after addition of CHX and subjected to SDS−PAGE and immunoblotting with anti-seipin antibody. Arrow, seipin; asterisk, cross-reacting band.

0.8 μg/mL pepstatin A, 0.8 μg/mL leupeptin, 8 μg/mL N^{α}-(*p*-toluenesulfonyl)-L-arginine methyl ester, 8 μg/mL N^{α}-tosyl-L-lysine chloromethyl ketone, 8 μg/mL benzoylarginine methyl ester,

and 8 μg/mL soybean trypsin inhibitor. Dounce homogenization was omitted following the 27000*g* centrifugation.

When necessary to apply to a glycerol or to a sucrose gradient, the sucrose in the partially purified ER was removed by first adding an equal volume of 20 mM HEPES/KOH, pH 7.4, 50 mM potassium acetate, 2 mM EDTA, 1 mM dithiothreitol (DTT), and protease inhibitors, which was mixed by pipetting, and then centrifuged at 60000 rpm in a Beckman TLA100.3 rotor (RCF_{av} = 152813*g*), 4 °C, 1 h, to pellet the microsomes.

Velocity Sedimentation and Gel Filtration. For gel filtration and the H_2O-based gradients, microsomal membranes were dissolved in 500 μL of 25 mM HEPES-NaOH, pH 7.5, with 150 mM NaCl, 0.5% Triton X-100, 1 mM DTT, and protease inhibitors as above. For the D_2O−sucrose gradients all buffer components except HEPES were constituted in D_2O instead of H_2O. A 1 M stock of HEPES−NaOH, pH 7.5, in H_2O was diluted with D_2O to 25 mM. Five hundred microliters of the identical buffer containing 15 μL of solubilized membranes and the following standards was applied to all gradients: 150−200 μg of porcine thyroglobulin, 27−100 μg of bovine liver catalase (omitted for seipin-mCherry, since it cross-reacted with DsRed antibody on blots), 36−100 μg of beef heart lactate dehydrogenase, and 30−40 μg of fraction V bovine serum albumin. The 10 mL gradients containing either 10−35% glycerol (v/v) or 5−20% sucrose (w/v) were centrifuged in an SW41 rotor at 35000 rpm 4 °C for 18−19 h for the H_2O-based gradients or 45−46 h for the D_2O−sucrose gradients. Fractions of 0.5 mL were harvested from the bottom of the gradients, and 19 μL of each was subjected to SDS gel electrophoresis and immunoblotting.

To determine the Stokes radius, solubilized membranes were loaded onto 80 or 90 mL Sephacryl S-500 HR columns which were calibrated with the molecular weight markers indicated above except 70S *E. coli* ribosomes or 40 nm diameter nanobeads were added. Dextran (MW 5−40 MDa) and glucose were markers of the void volume and column volume, respectively. Fractions were collected (ranging from 1.54 to 1.80 g samples in different runs) by gravity, and 19 μL of each fraction was subjected to SDS gel electrophoresis and immunoblotting. Standard proteins were detected by Amido Black-stained nitrocellulose, and both dextran and glucose were detected by phenol/H_2SO_4 (*17*). The nanobeads were detected by absorbance at 310 nm.

Calculation of the Molecular Mass of the Seipin Complex. To determine the mass of the seipin complex and the contribution of detergent, we combined methods mainly from Clark and Smigel (*18*) and Kumar et al. (*19*). A detailed description of the analytical methods leading to the determination of the hydrodynamic parameters of seipin is found in the Appendix.

Seipin Affinity Purification. Affinity purification was performed using the Pierce coimmunoprecipitation kit. One hundred microliters of AminoLink Plus resin were reacted with 373 μg of anti-myc antibody for conjugation according to the manufacturer's instructions and then diluted into 400 μL of coupling buffer. Yeast microsomes were dissolved in 400 μL of coupling buffer plus 0.5% Triton X-100 and protease inhibitors as above. The solution was cleared of particulate matter by centrifuging at 3000*g* for 1 min and then incubated with 40 μL beads overnight at 4 °C on a rocker. Seipin-myc13 was eluted with elution buffer as per the manufacturer's instructions except Triton X-100 was added to the neutralization buffer to 0.2% final concentration. To release seipin-TEVsite-myc13 from beads, they were incubated overnight at 4 °C with 8 μL of tobacco etch virus (TEV)-His_6 protease in 400 μL of 50 mM Tris-HCl, pH 7.5, 200 mM NaCl, 15% glycerol, 2 mM DTT, and 0.06% Triton X-100. Protein was recovered by centrifugation, and then the solution was subjected to nickel chromatography twice to remove the TEV-His_6.

Electron Microscopy of Purified Molecules. Carbon-coated 400-mesh copper grids were glowed discharged in air with 30 mA current for 1 min, and a 2.0 μL sample was loaded to a grid. After 30 s incubation, the grid was blotted with a piece of Whatman no. 4 filter paper, inverted, and incubated for 15−20 s on top of a drop of 120 μL of staining solution containing 6.0% ammonium molybdate/KOH, pH 6.4, and 0.5% trehalose and then blotted again to remove excess staining solution. The stained grids were dried in air for a couple of hours before examination in a JEOL 2200FS FEG transmission electron microscope. Images were taken with a 2K × 2K Tietz slow-scan CCD camera at a calibrated magnification of 56.3K and −1.5 μm defocus. A minimum-dosage system was used to limit the dose for every exposure to 20−30 electrons/$Å^2$.

Immunoblotting. Immunoblotting was performed with the ECL kit (Amersham). All primary antibodies were used at 1:1000 dilution except in Figures 1B and 5B and Supporting Information Figure S1, where anti-seipin antibody was used at 1:200.

RESULTS

Seipin Is in a Large Discrete Protein Complex. To determine whether seipin exists as a monomer or is in a larger complex, we initially prepared membranes from a cell line that overexpressed (using the *PGK1* promoter on a low copy plasmid) yeast seipin tagged at its carboxy terminus with mCherry. We had previously shown that seipin-mCherry in these cells correctly targets to the ER (*6*). Membrane proteins were solubilized with Triton X-100, and the extract was subjected to centrifugation through a detergent glycerol gradient. Seipin-mCherry (59.7 kDa predicted MW) was detected in a discrete peak just behind the thyroglobulin (669 kDa) internal standard and well ahead of lactate dehydrogenase (140 kDa), suggesting that it forms a complex with other proteins (Figure 1A). To determine if the mCherry tag was necessary for complex formation, we generated an anti-peptide antibody against yeast seipin. Although it could not detect endogenous protein, overexpressed (using the *PGK1* promoter) untagged protein was easily detected. Again, seipin was detected only in a large complex as a discrete species. Seipin behaved on SDS gels as a 27 kDa protein instead of 32 kDa predicted from its sequence. However, the primary translation product from an in vitro transcription−translation system also behaved as a 27 kDa species (Supporting Information Figure S1), suggesting that seipin migrates more rapidly than predicted through Laemmli gels.

To rule out an overexpression artifact, we tagged seipin in the chromosome (so that its endogenous promoter was used) with 13 tandem copies of the myc epitope. (Two copies were insufficient for detection; data not shown.) Again, seipin behaved on a glycerol detergent gradient as a discrete species, migrating close to the soluble marker catalase (250 kDa), although its monomer molecular mass was 52.9 kDa. Some degradation of seipin-myc13, forming a ladder of species that corresponded to proteolytic removal of a varying number of myc epitopes, was always seen, even in extracts from cells killed in acid (Figure 1A and data not shown). Overexpression of seipin-myc13 using the *PGK1* promoter on a plasmid yielded an identical migration in the glycerol gradients (Figure 1A), suggesting that there were no limiting components in the complex other than seipin. The complex was stable, since

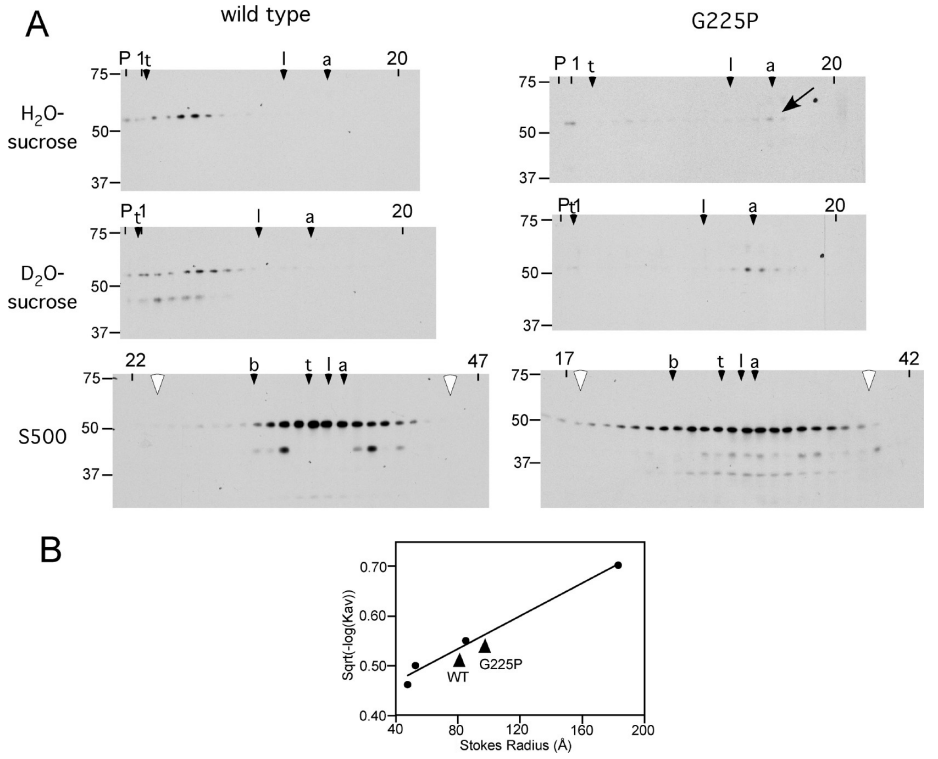

FIGURE 2: Hydrodynamic behavior of seipin-mCherry and seipin[G225P]-mCherry. (A) Rows 1 and 2: Immunoblots of fractions from detergent H_2O- or D_2O-sucrose gradients of seipin-mCherry ("wild-type" column) and seipin[G225P]-mCherry ("G225P" column). See legend to Figure 1 for more details. Arrow indicates the G225P form, which is difficult to visualize. Row 3: Immunoblots of fractions from S500 chromatography. White arrowheads on each blot indicate void volume, left, and column volume, right. Native markers identical to Figure 1 except b, 5 nm nanobeads. (B) Curve of Stokes radii of standards from S500, with arrow indicating behavior of seipin[G225P]-mCherry ("G225P").

the protein, isolated from peak fractions and subjected to a second glycerol gradient, migrated identically (data not shown).

To determine whether seipin maintained its discrete oligomeric form in other detergents, we solubilized membranes containing seipin-myc13 (expressed from the endogenous promoter in the chromosome) in the nonionic detergents dodecyl octaethylene glycol ether ($C_{12}E_8$) or dodecyl β-D-maltoside (DDM), the zwitterionic detergent CHAPS, or the anionic detergent sodium cholate and then subjected the extract to glycerol gradient centrifugation in the same detergents. Regardless of the detergent used, seipin-myc13 migrated as a discrete oligomeric species (Supporting Information Figure S2A). Its apparent molecular mass (compared to the internal soluble standards) varied from 200 or 400 kDa, but it was negatively correlated with the partial specific volume of the detergent (Supporting Information Figure S2B), suggesting that the buoyancy of the detergent rather than the number of monomers in the complex was more important to the different migration rates.

Yeast seipin mutated at residue 225 from glycine to proline (G225P) is orthologous to the missense human seipin A212P that is a cause of lipodystrophy (*6*). Untagged seipin[G225P] overexpressed from the *PGK1* promoter could not be detected by our seipin antibody on these gradients (Figure 1A), suggesting that the protein is unstable (the epitope is distant from G225), since the wild-type form was easily detected. In whole cell lysates, however, overexpressed untagged seipin[G225P] could be observed, albeit at lower levels than wild type (Figure 1B, compare with upper cross-reacting band). Upon addition of cycloheximide, the mutated form demonstrated a half-life of about 1 h, whereas little wild-type seipin disappeared after 6 h. Seipin[G225P] was partially stabilized by the proteosomal inhibitor MG132, indicating a route for its degradation.

In contrast to untagged seipin[G225P], both the overexpressed seipin[G225P]-mCherry and even the chromosomally expressed (using the endogenous promoter) seipin[G225P]-myc13 were detected, albeit at levels lower than the unmutated analogues, indicating that carboxy-terminal tags may stabilize the G225P forms to some extent. Nevertheless, seipin[G225P]-mCherry and seipin[G225P]-myc13 migrated much more slowly in detergent glycerol gradients than their wild-type counterparts, suggesting that they can form only smaller complexes.

Tagged Seipins Are in an ~500 kDa Protein Complex. Although detergent glycerol gradient centrifugation indicates that seipin is in a large complex, this technique cannot be used to determine the size of the complex since bound detergent used to extract seipin will change its hydrodynamic properties. Thus the internal water-soluble standards in the glycerol gradients are inaccurate for gauging the size of seipin. However, the molecular mass of both a protein−detergent complex and the protein component alone can be determined if the following attributes of a discrete protein−detergent complex are known: the Stokes radius, the partial specific volume (ν), and the sedimentation coefficient extrapolated to standard conditions ($s_{20,w}$) (*20*, *21*). These constants were determined for both seipin and seipin[G225P] tagged with either mCherry (overexpressed) or with myc13 (expression driven by the endogenous chromosomal promoter). Briefly (see Appendix for details), the Stokes radii were determined from Sephacryl S500 exclusion chromatography using standards with known Stokes radii. Values for ν were determined from H_2O- and D_2O-sucrose gradient velocity sedimentation, and finally these values were used to calculate $s_{20,w}$ using standards with known $s_{20,w}$. Behaviors of the mCherry-tagged seipins after the sucrose gradients and S500 columns are shown in Figure 2A and

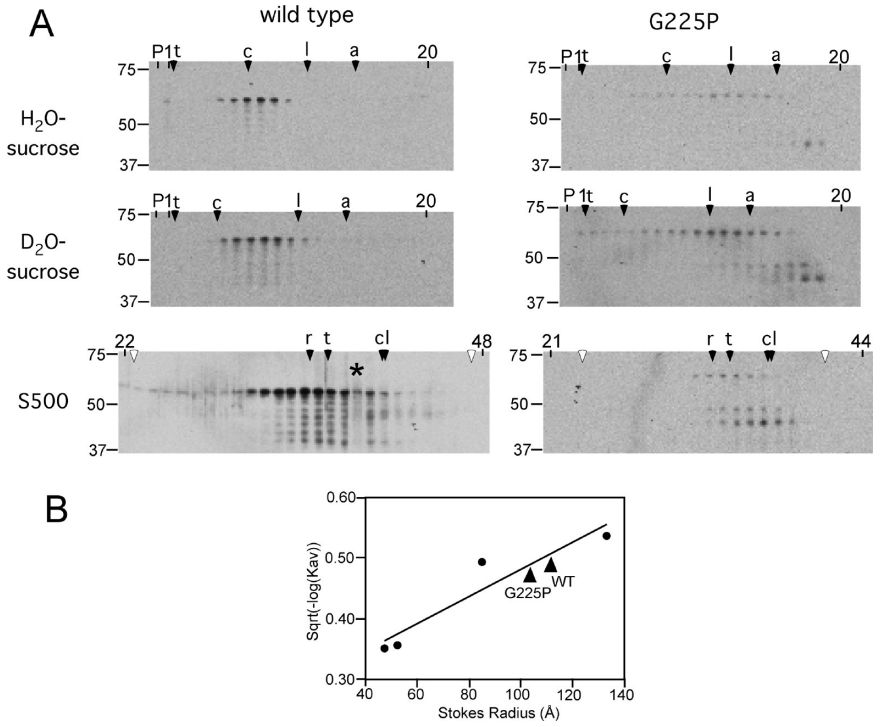

FIGURE 3: Hydrodynamic behavior of seipin-myc13 and seipin[G225P]-myc13. Identical to Figure 2 except seipins were tagged with 13 tandem copies of the myc epitope (in the chromosome to use the endogenous promoter) instead of overexpressing seipin-mCherry forms on plasmids, and we used 70S *E. coli* ribosomes "r" instead of beads as a marker. "*", much of this fraction was lost during processing.

Table 2: Seipin and MW Standard Physical Attributes

protein	ν^a (mL/g)	$s_{20,w}{}^b$	Stokes radius (Å)	$M_c{}^c$ (kDa)	detergent/protein oligomer^d	$M_p{}^e$ (kDa)	subunits/complex
seipin-myc13	0.776 ± 0.015^f	11.1 ± 0.7	113	640 ± 80	222	498 ± 5.5	9.4
[G225P]-myc13	0.783 ± 0.033	8.0 ± 1.1	104	454 ± 127	214	316 ± 6	6.0
seipin-mCherry	0.769 ± 0.0043	15.6 ± 0.34	80.9	620 ± 3.5	160	517 ± 19	8.7
[G225P]-mCherry	0.772 ± 0.015	4.78 ± 0.30	97.5	233 ± 29.5	70	188 ± 3	3.1
BSA^g	0.734	4.31	ND				
LDH	0.747	7.45	47.5				
catalase	0.730	11.3	52.2				
thyroglobulin	0.723	19.3	85				
70S ribosomes	NA	NA	133				
40 nm nanobeads	NA	NA	183^h				

^{a}Partial specific volume and ^{b}Svedberg coefficient (in S units): for seipin forms they refer to the protein−detergent complex; for the standards they refer to the purified proteins. ^{c}Calculated molecular mass of the seipin oligomer−detergent complex. ^{d}Moles of Triton X-100 bound to a mole of seipin oligomer. ^{e}Calculated molecular mass of the protein component of the detergent complex. $^f x \pm y$ throughout the table denotes mean and range from two preparations. ^{g}See Appendix for references regarding these standards. ^{h}Measured average radius of the nanobeads according to the manufacturer.

for myc13-tagged seipins in Figure 3A. Interpolation of Stokes radii of the tagged seipins based on the behavior of standards through the S500 column is shown in panel B of these figures.

The results of this analysis are shown in Table 2. The seipin-myc13 detergent complex was calculated to have a molecular mass of 640 kDa containing a protein component of 498 kDa. Similarly, these parameters for seipin-mCherry were 620 and 517 kDa. In contrast, the main species of seipin[G225P]-myc13 and -mCherry were calculated to have protein components of 316 and 188 kDa, respectively. There was not a corresponding decrease in the Stokes radii between wild-type and [G225P] forms. However, all of the values were close to the Stokes radius of a Triton X-100 micelle, 95 Å (*22*), so this parameter may reflect the detergent contribution to the complex more than the core protein. Regardless, from the protein molecular weight analysis we conclude that the G225P mutation does not allow seipin to form normal complexes, although it can form smaller ones.

Seipin Forms Homooligomers. Preliminary experiments failed to find heterologous partners in seipin complexes. To determine if seipin can self-associate, we performed a mixing experiment: low levels of seipin-myc13 (produced from the endogenous seipin promoter) were expressed with higher levels of either seipin-mCherry or seipin[G225P]-mCherry (using the *PGK1* promoter). If seipin can self-associate, the behavior of seipin-myc13 on glycerol gradients should be influenced by overexpression of mCherry-tagged forms. Indeed, this was the case: seipin-myc13 was shifted to smaller molecular weight when coexpressed with seipin-[G225P]-mCherry compared to the wild-type seipin-mCherry (Figure 4). This result indicates that seipin can self-associate.

To determine if seipin is a homooligomer, we affinity purified seipin-myc13 from solubilized membranes after adding a tobacco etch virus (TEV) protease cleavage site between the seipin coding sequence and the myc13 tag (Figure 5). We used anti-myc Sepharose for the purification, and solubilized membranes from wild-type

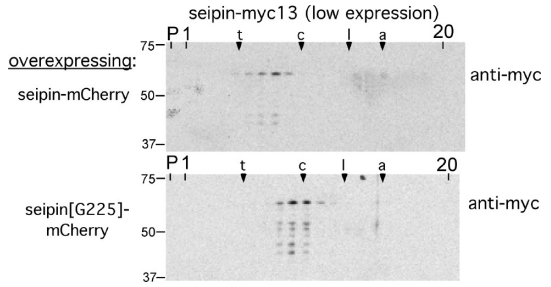

FIGURE 4: Seipin can self-associate. Anti-myc immunoblots from detergent glycerol gradients. Besides expressing seipin-myc13 from the endogenous chromosomal promoter, cells also oveexpressed either seipin-mCherry (top row) or seipin[G225P]-mCherry (bottom row). See legend to Figure 1 for more details. Note the shift in the complex to lower MW when coexpressed with seipin[G225P]-mCherry.

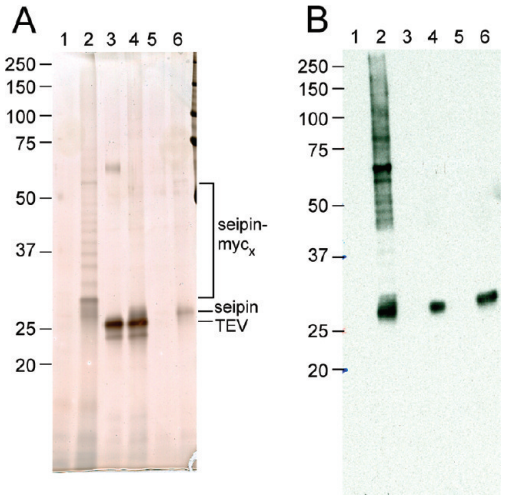

FIGURE 5: Seipin is a homooligomer. ER-enriched membranes from wild type (lanes 1, 3, and 5) or the seipin-myc13-overexpressing strain (lanes 2, 4, and 6) were solubilized in detergent and incubated with anti-myc epitope antibody-conjugated beads. Protein was eluted with elution buffer (from manufacturer) (lanes 1 and 2) or eluted with TEV protease (lanes 3−6). Protease was removed on a nickel column (lanes 5 and 6). Samples were subjected to SDS−PAGE and stained with silver (A) or immunoblotted with anti-seipin antibody (B). The migration of the seipin-myc$_x$ ladder, seipin, and TEV protease are indicated in (A).

cells were processed in parallel as a negative control. Protein was eluted from the beads either by elution buffer supplied by the manufacturer or after incubation with polyhistidine-tagged TEV protease. Using the acidic elution buffer instead of TEV resulted in a regularly spaced ladder of protein bands consistent with cleavage of varying numbers of myc epitope copies during the processing (similar to the myc ladders observed after gradient fractionation in Figures 3 and 4) and marked as "seipin-myc$_x$" in Figure 5. We found that more TEV was required for elution than expected, probably since a homooligomer would require cleavage at several sites for elution. Subsequently, the protease was removed on a nickel column, resulting in a single major band visible by protein staining with silver that cross-reacted with anti-seipin antibody. Although we cannot yet rule out substoichiometric constituents of seipin, we conclude that seipin is predominantly a homooligomer. Considering the size of the protein complex, we estimate nine subunits per complex (calculated at 9.4 and 8.7 for seipin-myc13 and seipin-mCherry, Table 2).

Seipin Resembles a Toroid. Affinity-purified seipin-myc13 was subjected to negative staining electron microscopy. Both proteins eluted from the affinity beads by elution buffer and after TEV protease incubation were imaged. Both appear as disks with radii of 5.33 and 5.44 nm, respectively (Figure 6A,C). The disks appear to have a hollow center and form toroids, which is more apparent in Figure 6A, although more structural studies will be required to confirm this shape. There were no particles present in parallel samples from cells not expressing seipin-myc13 (Figure 6 B).

DISCUSSION

This is the first report of seipin purification or seipin structure. Seipin is predicted to cross the ER membrane twice with termini facing the cytosol; this topology appears likely since the loop region is glycosylated, in mammals and glycosylation sites engineered at the termini (distal from the two predicted transmembrane domains) are not used (*9*). We now add to this model by demonstrating that seipin is a homooligomer of about nine subunits that appears to form toroids. While we only purified and determined the oligomeric state of tagged seipin, the mCherry and myc13 fusions we studied complement the null mutation, even when introduced under the endogenous chromosomal promoter (ref *6* and data not shown) indicating that they are active. The oligomer is also stable and does not dissociate even after two successive centrifugations on glycerol gradients. Oligomers solubilized in various detergents migrate differently in glycerol gradients (Supporting Information Figure S2), but this appears to be largely an effect of the different detergent buoyancies. Additional experiments will be required to determine if the oligomers from different extraction methods have more subtle differences which may yield clues of function.

While the phenotype of human seipin[A212P] resembles that from other nonsense alleles, the reason for this has been unknown. Here we show that the orthologous missense mutation in yeast, G225P, is quite unstable and cannot be detected on gradients even when overexpressed from the *PGK1* promoter. Stability is increased with the addition of the myc13 or mCherry tags to the carboxy terminus. However, only smaller homooligomers can be formed with the G225P mutation: estimated at a hexamer for seipin[G225P]-myc13 or a trimer with seipin[G225P]-mCherry. This behavior may indicate that seipin is assembled from trimers. Regardless of assembly mechanism, our data suggest that human seipin[A212P] is unstable because it cannot form the normal ~nonomeric structure.

While the Stokes radius of seipin-myc13 is 113 Å, the radius by negative staining is only 53 Å. This difference might be caused by the behavior of the unstructured tandem myc epitopes on the gel filtration column compared with negative staining, where it may be difficult to image, since the size of the particles by this method was identical with or without the epitope tag. The 2-fold difference might also have been caused by effects of the detergent in these two systems (0.5% Triton was used for gel filtration, 0.06% for negative staining) or shrinkage of protein on the grid. Further work will be required to sort this out. Regardless, we now are poised to computer average many seipin images to obtain a more resolved structure.

Our data do not address the contact sites on seipin that are required to form the oligomer. While the simplest model based on the presumed topology of seipin is one in which interactions occur principally through the transmembrane domains (the termini beyond these domains are very short in yeast), the inability of the G225P to correctly assemble suggests that the loop domain is involved in contact sites between the monomers such that this

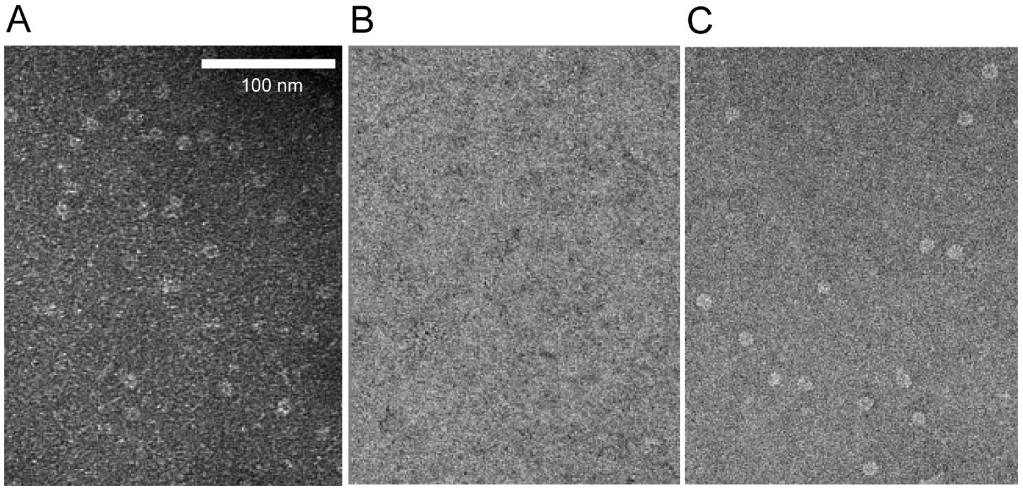

FIGURE 6: Seipin forms a toroid. Negative staining of (A) affinity-purified seipin-myc13 from overexpressing cells, eluted from antibody column with elution buffer from the manufacturer. (B and C) Affinity-purified seipin-TEVsite-myc13 (C) eluted with TEV protease or a parallel sample from nonexpressing cells (B).

mutation disrupts them. To address this question, we will express the loop domain alone (with signals to target it to the ER lumen) to determine if it can bind to full-length seipin.

The challenge in determining seipin function may be in dissecting direct from indirect effects. The three principal phenotypes of seipin-null cells are changes in droplet morphology and behavior (i.e., shape, apparent chaotic budding of droplets from the ER, and ability to undergo homotypic fusion), resulting changes in lipid composition and amounts, and a block in adipogenesis (*5*, *6*, *10*−*12*). Our hypothesis, strengthened from the seipin structure presented here, is that seipin is involved in organizing droplets, perhaps in part by forming a collar at the ER−droplet interface or by preventing droplets from evaginating into the lumen. We suspect that as an organizer it facilitates trafficking of lipids and/or proteins between these two compartments. Seipin is not necessary for droplet formation, suggesting to us that droplets can occur spontaneously; it is unclear whether droplets in seipin-deficient cells are functional in terms of mobilizing lipid. We imagine that changes in lipid profiles that occur in the absence of functional seipin are secondary responses, as is the decision of preadipocytes (but not fibroblasts and other cells) to abort adipogenesis if droplets are not correctly assembled. An exploration to determine if seipin structure extends beyond the core oligomer reported here might be a productive avenue to more directly address seipin function.

ACKNOWLEDGMENT

We thank Susan Ferro-Novick (UC San Diego) for the pFA6-13myc-HIS3MX6 vector used to tag seipin, Jamie Cate and Jack Dunkle (UC Berkeley) for *E. coli* 70S ribosomes used as a gel filtration standard, and George DeMartino (UT Southwestern) for MG132. We are grateful to Hui Zheng for technical assistance in electron microscopic negative staining, Bing Li for help with in vitro transcription−translation, and the Goodman laboratory for useful discussions.

APPENDIX

Hydrodynamic Parameters of Seipin. Our procedures combine previous methods (*18*, *20*−*23*). The mass of the seipin protein complex (M_p) can be determined knowing the mass of the protein/detergent complex (M_c) and the partial specific volumes of the protein, the protein/detergent complex, and the detergent (ν_p, ν_c, and ν_d, respectively) according to the equation

$$M_p = M_c/(1 + (\nu_p - \nu_c)/(\nu_c - \nu_d)) \quad (1)$$

The M_c can be determined with the equation

$$M_c = 6\pi N \eta_{20,w} A_c s_{20,w}/(1 - \nu_c \rho_{20,w}) \quad (2)$$

where N is Avogadro's number, $\eta_{20,w}$ and $\rho_{20,w}$ are the viscosity and density, respectively, of water under standard conditions (1.002 cP and 0.99823 g/mL), and A_c and $s_{20,w}$ are the Stokes radius and the sedimentation constant under standard conditions, respectively, of the seipin protein/detergent complex. To solve for M_c and M_p we determined the Stokes radius, the partial specific volume, and the sedimentation coefficient under standard conditions of the seipin protein/detergent complex.

The Stokes radius was determined from a standard curve of elution volumes of proteins with known Stokes radii (Table 2). For each standard, a value was calculated for $K_{av} = (V_e - V_0)/(V_c - V_0)$, where V_e is the elution volume, V_c is the column volume (determined with glucose), and V_0 is the void volume (determined with dextran 5−40 MDa (Sigma)). For the nanobead standard, the Stokes radius was assumed equal to half the mean number diameter according to the manufacturer. A linear regression was calculated for a plot of $(-\log(K_{av}))^{1/2}$ vs Stokes radius for the standards from which the Stokes radius (A_c) for the seipin protein/detergent complex was determined.

The partial specific volume, ν_c, was determined from the position of the seipin protein/detergent complex in sucrose gradient centrifugation using the equation

$$\nu_c = (S_D \eta_D/S_H \eta_H - 1)/(\rho_H (S_D \eta_D/S_H \eta_H) - \rho_D) \quad (3)$$

where S, η, and ρ refer to the sedimentation coefficient, of the complex, and the viscosity and density, respectively, of the medium at the peak radial position of seipin and H and D subscripts refer to sucrose gradients in H_2O and D_2O, respectively. S was determined in each gradient using the equation

$$S = ((r_{peak} - r_0)/t)/\omega^2 r_{avg}$$

where r_0 is the position from the center of rotation of the top of the gradient, ω is the angular velocity ($= 2\pi(\text{rpm})/60$), t is time of centrifugation, and $r_{avg} = (r_{peak} + r_0)/2$.

The values for ρ in the gradients corresponding to the peaks of the complex (for eq 3) were interpolated from the density of the two solutions used to mix the gradient at the position of seipin, assuming a linear gradient of density from the top to bottom of the gradient. For viscosity (η) we cannot assume linearity in the gradient. Therefore, we used internal protein standards with known $s_{20,w}$ values to determine the viscosity of the gradient at the position of each standard by the formula

$$\eta = \eta_{20,w}(s_{20,w}/S)(1-\nu\rho)/(1-\nu\rho_{20,w})$$

where $\eta_{20,w}$ and $\rho_{20,w}$ are the viscosity and density of water, as above. Values for standards are shown in Table 2 and are based on the following references: BSA (*24*, *25*), LDH (*26*, *27*), catalase (*28*−*33*), thyroglobulin (*31*, *34*−*37*), and 70S ribosomes (*37*, *38*). From these graphs of $s_{20,w}$ vs viscosity we interpolated values of η at the position of the seipin complex and solved eq 3 for ν_c.

From these data, the $s_{20,w}$ for the seipin protein/detergent complex can be determined using the formula

$$s_{20,w} = S_H(\eta_H/\eta_{20,w})(1-\nu_c\rho_{20,w})/(1-\nu_c\rho_c)$$

where ρ_c refers to the density at the peak radial position for the seipin protein/detergent complex for the H_2O gradient. (A similar formula can be used for the D_2O gradient, which should yield the identical value.)

Having determined A_c, ν_c, and $s_{20,w}$ for the protein/detergent complex, its molecular mass was determined using eq 2 and 0.908 for the partial specific volume for Triton X-100 (ν_d) (*23*). Finally, the protein component of the complex was calculated using eq 1. Results are shown in Table 2.

SUPPORTING INFORMATION AVAILABLE

Figure S1 comparing the migration by SDS−PAGE of seipin from cells and from in vitro translation, Figure S2 comparing the behavior of seipin, extracted with five different detergents, after glycerol gradient centrifugation, and corresponding methods and references accompanying the figures. This material is available free of charge via the Internet at http://pubs.acs.org.

REFERENCES

1. Garg, A. (2004) Acquired and inherited lipodystrophies. *N. Engl. J. Med. 350*, 1220–1234.
2. Simha, V., and Garg, A. (2009) Inherited lipodystrophies and hypertriglyceridemia. *Curr. Opin. Lipidol. 20*, 300–308.
3. Oral, E. A., and Chan, J. L. (2010) The rationale for leptin-replacement therapy as a treatment for severe lipodystrophy. *Endocr. Pract.*, 1–35.
4. Magre, J., Delepine, M., Khallouf, E., Gedde-Dahl, T., Jr., Van Maldergem, L., Sobel, E., Papp, J., Meier, M., Megarbane, A., Bachy, A., Verloes, A., d'Abronzo, F. H., Seemanova, E., Assan, R., Baudic, N., Bourut, C., Czernichow, P., Huet, F., Grigorescu, F., de Kerdanet, M., Lacombe, D., Labrune, P., Lanza, M., Loret, H., Matsuda, F., Navarro, J., Nivelon-Chevalier, A., Polak, M., Robert, J. J., Tric, P., Tubiana-Rufi, N., Vigouroux, C., Weissenbach, J., Savasta, S., Maassen, J. A., Trygstad, O., Bogalho, P., Freitas, P., Medina, J. L., Bonnicci, F., Joffe, B. I., Loyson, G., Panz, V. R., Raal, F. J., O'Rahilly, S., Stephenson, T., Kahn, C. R., Lathrop, M., and Capeau, J. (2001) Identification of the gene altered in Berardinelli-Seip congenital lipodystrophy on chromosome 11q13. *Nat. Genet. 28*, 365–370.
5. Fei, W., Shui, G., Gaeta, B., Du, X., Kuerschner, L., Li, P., Brown, A. J., Wenk, M. R., Parton, R. G., and Yang, H. (2008) Fld1p, a functional homologue of human seipin, regulates the size of lipid droplets in yeast. *J. Cell Biol. 180*, 473–482.
6. Szymanski, K. M., Binns, D., Bartz, R., Grishin, N. V., Li, W. P., Agarwal, A. K., Garg, A., Anderson, R. G., and Goodman, J. M. (2007) The lipodystrophy protein seipin is found at endoplasmic reticulum lipid droplet junctions and is important for droplet morphology. *Proc. Natl. Acad. Sci. U.S.A. 104*, 20890–20895.
7. Windpassinger, C., Auer-Grumbach, M., Irobi, J., Patel, H., Petek, E., Horl, G., Malli, R., Reed, J. A., Dierick, I., Verpoorten, N., Warner, T. T., Proukakis, C., Van den Bergh, P., Verellen, C., Van Maldergem, L., Merlini, L., De Jonghe, P., Timmerman, V., Crosby, A. H., and Wagner, K. (2004) Heterozygous missense mutations in BSCL2 are associated with distal hereditary motor neuropathy and Silver syndrome. *Nat. Genet. 36*, 271–276.
8. Ito, D., and Suzuki, N. (2007) Molecular pathogenesis of seipin/BSCL2-related motor neuron diseases. *Ann. Neurol. 61*, 237–250.
9. Lundin, C., Nordstrom, R., Wagner, K., Windpassinger, C., Andersson, H., von Heijne, G., and Nilsson, I. (2006) Membrane topology of the human seipin protein. *FEBS Lett. 580*, 2281–2284.
10. Chen, W., Yechoor, V. K., Chang, B. H., Li, M. V., March, K. L., and Chan, L. (2009) The human lipodystrophy gene product Berardinelli-Seip congenital lipodystrophy 2/seipin plays a key role in adipocyte differentiation. *Endocrinology 150*, 4552–4561.
11. Payne, V. A., Grimsey, N., Tuthill, A., Virtue, S., Gray, S. L., Dalla Nora, E., Semple, R. K., O'Rahilly, S., and Rochford, J. J. (2008) The human lipodystrophy gene BSCL2/seipin may be essential for normal adipocyte differentiation. *Diabetes 57*, 2055–2060.
12. Boutet, E., El Mourabit, H., Prot, M., Nemani, M., Khallouf, E., Colard, O., Maurice, M., Durand-Schneider, A. M., Chretien, Y., Gres, S., Wolf, C., Saulnier-Blache, J. S., Capeau, J., and Magre, J. (2009) Seipin deficiency alters fatty acid Delta9 desaturation and lipid droplet formation in Berardinelli-Seip congenital lipodystrophy. *Biochimie 91*, 796–803.
13. Ito, H., Fukuda, Y., Murata, K., and Kimura, A. (1983) Transformation of intact yeast cells treated with alkali cations. *J. Bacteriol. 153*, 163–168.
14. Liu, C., Apodaca, J., Davis, L. E., and Rao, H. (2007) Proteasome inhibition in wild-type yeast *Saccharomyces cerevisiae* cells. *BioTechniques 42*, 158–162.
15. Amberg, D. C., Burke, D. J., and Strathern, J. N. (2005) Methods in Yeast Genetics, 2005 ed., Cold Spring Harbor Laboratory Press, Cold Spring Harbor, NY.
16. Shimoni, Y., and Schekman, R. (2002) Vesicle budding from endoplasmic reticulum. *Methods Enzymol. 351*, 258–278.
17. Geater, C. W., Fehr, W. R., Wilson, L. A., and Robyt, J. F. (2001) A more rapid method of total sugar analysis for soybean seed. *Crop Sci. 41*, 250–252.
18. Clarke, S., and Smigel, M. D. (1989) Size and shape of membrane protein-detergent complexes: hydrodynamic studies. *Methods Enzymol. 172*, 696–709.
19. Kumar, K. N., Eggeman, K. T., Adams, J. L., and Michaelis, E. K. (1991) Hydrodynamic properties of the purified glutamate-binding protein subunit of the N-methyl-D-aspartate receptor. *J. Biol. Chem. 266*, 14947–14952.
20. Clarke, S. (1975) The size and detergent binding of membrane proteins. *J. Biol. Chem. 250*, 5459–5469.
21. Reynolds, J. A., and Tanford, C. (1976) Determination of molecular weight of the protein moiety in protein-detergent complexes without direct knowledge of detergent binding. *Proc. Natl. Acad. Sci. U.S.A. 73*, 4467–4470.
22. Helenius, A., and Simons, K. (1975) Solubilization of membranes by detergents. *Biochim. Biophys. Acta 415*, 29–79.
23. Tanford, C., and Reynolds, J. A. (1976) Characterization of membrane proteins in detergent solutions. *Biochim. Biophys. Acta 457*, 133–170.
24. Creeth, J. M. (1952) The use of the Gouy diffusiometer with dilute protein solutions: an assessment of the accuracy of the method. *Biochem. J. 51*, 10–17.
25. Edsall, J. T. (1953−1954) The Size, Shape and Hydration of Protein Molecules, Vol. 1B, Academic Press, New York.
26. Haga, T., Haga, K., and Gilman, A. G. (1977) Hydrodynamic properties of the beta-adrenergic receptor and adenylate cyclase from wild type and varient S49 lymphoma cells. *J. Biol. Chem. 252*, 5776–5782.
27. Pesce, A., McKay, R. H., Stolzenbach, F., Cahn, R. D., and Kaplan, N. O. (1964) The comparative enzymology of lactic dehydrogenases. I. Properties of the crystalline beef and chicken enzymes. *J. Biol. Chem. 239*, 1753–1761.
28. Brewer, J. M., Ljungdahl, L., Spencer, T. E., and Neece, S. H. (1970) Physical properties of formyltetrahydrofolate synthetase from *Clostridium thermoaceticum*. *J. Biol. Chem. 245*, 4798–4803.
29. Dobao, M., Castillo, F., and Pineda, M. (1993) Characterization of urease from the phototrophic bacterium *Rhodobacter capsulatus* E1F1. *Curr. Microbiol. 27*, 119–123.
30. Richie-Jannetta, R., Francis, S. H., and Corbin, J. D. (2003) Dimerization of cGMP-dependent protein kinase Ibeta is mediated by an extensive amino-terminal leucine zipper motif, and dimerization modulates enzyme function. *J. Biol. Chem. 278*, 50070–50079.

31. Rogers, K. S., Rodwell, V. W., and Geiger, P. (1997) Active form of *Pseudomonas mevalonii* 3-hydroxy-3-methylglutaryl coenzyme A reductase. *Biochem. Mol. Med. 61*, 114–120.
32. Sumner, J. B., and Gralen, N. (1938) The molecular weight of crystalline catalase. *J. Biol. Chem. 125*, 33–36.
33. Unsal-Kacmaz, K., and Sancar, A. (2004) Quaternary structure of ATR and effects of ATRIP and replication protein A on its DNA binding and kinase activities. *Mol. Cell. Biol. 24*, 1292–1300.
34. CRC (1989) CRC Practical Handbook of Biochemistry and Molecular Biology, CRC Press, Boca Raton, FL.
35. Derrien, Y., Michel, R., Pederson, K. O., and Roche, J. (1949) Recherches sur la preparation et sur les proprietes de la thyroglobuline pure. II. *Biochim. Biophys. Acta 3*, 436–441.
36. Heidelberger, M., and Pederson, K. O. (1935) The molecular weight and isoelectric point of thyroglobulin. *J. Gen. Physiol. 19*, 95–108.
37. Ohashi, T., Ishimizu, T., Akita, K., and Hase, S. (2007) In vitro stabilization and minimum active component of polygalacturonic acid synthase involved in pectin biosynthesis. *Biosci., Biotechnol., Biochem. 71*, 2291–2299.
38. Amand, B., Pochon, F., and Lavalette, D. (1977) Rotational diffusion of *Escherichia coli* ribosomes. I. Free 70 S, 50 S, and 30 S particles. *Biochimie 59*, 779–784.
39. Sikorski, R. S., and Hieter, P. (1989) A system of shuttle vectors and yeast host strains designed for efficient manipulation of DNA in *Saccharomyces cerevisiae*. *Genetics 122*, 19–27.